

AUTOREGRESSIVE SIGN LANGUAGE PRODUCTION: A GLOSS-FREE APPROACH WITH DISCRETE REPRESENTATIONS

Eui Jun Hwang, Huije Lee, Jong C. Park[†]

Korea Advanced Institute of Science and Technology (KAIST), Daejeon, Korea

ABSTRACT

Gloss-free Sign Language Production (SLP) offers a direct translation of spoken language sentences into sign language, bypassing the need for gloss intermediaries. This paper presents the Sign language Vector Quantization Network, a novel approach to SLP that leverages Vector Quantization to derive discrete representations from sign pose sequences. Our method, rooted in both manual and non-manual elements of signing, supports advanced decoding methods and integrates latent-level alignment for enhanced linguistic coherence. Through comprehensive evaluations, we demonstrate superior performance of our method over prior SLP methods and highlight the reliability of Back-Translation and Fréchet Gesture Distance as evaluation metrics.

Index Terms— Sign language production, vector quantization, autoregression

1. INTRODUCTION

Gloss-free Sign Language Production (SLP) directly translates spoken language into sign poses, eschewing the needs for glosses. Glosses, essentially unique identifiers for individual signs, provide a direct link between spoken language and sign poses. However, they demand intricate annotations by Sign Language (SL) experts and often miss the subtle intricacies of SL expressions, particularly the manual and non-manual signals [1, 2].

In the domain of gloss-free SLP, two main approaches prevail: retrieval and generative models. Retrieval models [3–5] fetch relevant samples from datasets based on textual prompts. Generative models [6–8], on the other hand, can create entirely new signing sequences by leveraging patterns learned during training. This capability to produce diverse outputs makes generative models a compelling choice for SLP, which is the focus of our research. However, the generative models face a few challenges. The length disparity between sign pose sequences and their spoken equivalents often necessitates clustering sequences into gloss-level representations [2]. Moreover, crafting spatio-temporal motions that maintain syntactic and semantic coherence in SL is com-

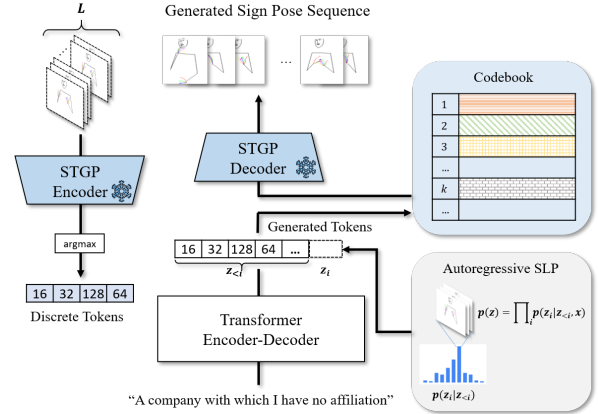


Fig. 1. An overview of SignVQNet. The STGP encoder transforms continuous sign poses into discrete tokens. These tokens are then generated from textual inputs by the Transformer. Subsequently, the STGP decoder converts the generated tokens back into actual sign pose sequences.

plex, especially when contrasted with the linear structure of spoken language.

Recent studies [8, 9] have pointed out the constraints of the model introduced in [6]. A significant concern is its dependence on the initial ground-truth pose and timing for inference, pivotal for the model’s autoregression. This reliance indicates that true autoregressive generation for continuous datasets, such as sign poses, might be intricate without such auxiliary information during inference.

To address this, we introduce Sign language Vector Quantization Network (SignVQNet), as shown in Fig. 1. By leveraging Vector Quantization (VQ), SignVQNet captures discrete tokens from continuous sign poses. This enables genuine autoregressive generation, introducing the discrete tokens that function without the need for auxiliary information during inference. This approach also supports beam search, commonly used for Natural Language Processing (NLP), and introduces latent-level alignment to directly associate linguistic features with sign pose features.

We evaluated the performance of SignVQNet against other existing SLP models using Back-Translation (BT), DTW-MJE, and Fréchet Gesture Distance (FGD). The results

[†]Corresponding author, park@nlp.kaist.ac.kr

show that SignVQNet consistently outperformed its counterparts. However, our analysis revealed that DTW-MJE suffers from inconsistencies, raising questions about its reliability as a suitable metric for SLP. On the other hand, both BT and FGD proved to be more consistent and reliable in our evaluations.

2. RELATED WORKS

Generative Gloss-free SLP. Saunders et al. [6] pioneered the application of Progressive Transformers (PT) to gloss-free SLP. Their approach combined a unique counter decoding method and augmentation strategies such as Gaussian Noise and Future Prediction. Additionally, they introduced a back translation evaluation metric to assess model performance. Building on this, Saunders et al. [10] addressed the regression-to-the-mean issue by adopting an adversarial training framework. In a subsequent work, Saunders et al. [7] optimized PT by employing a mixture of motion primitives. Meanwhile, Hwang et al. [8] introduced a paradigm shift with their Non-Autoregressive Sign Language Production with Gaussian space (NSLP-G) model. Designed to convert spoken language sentences into corresponding sign pose sequences, NSLP-G diverged from conventional methods by adopting non-autoregressive decoding and implementing a two-phase approach to the SLP task.

Discrete Representation. Several studies have focused on converting continuous data into discrete forms. Maddison et al. [11] and Jang et al. [12] developed methods for approximating discrete sampling from continuous distributions. Van et al. [13] enhanced autoencoders with a discrete codebook in VQ-VAE, aligning encoder outputs to the nearest codebook vector. Gumbel-Softmax relaxation, in particular, has proven effective for learning discrete latent distributions [14]. In our work, we utilize this method to discretize sign poses.

3. METHOD

Problem Formulation. Consider a textual input $x = \{x_u\}_{u=1}^U$, consisting of U words. The objective of SLP is to produce a continuous signing sequence $y = \{y_t\}_{t=1}^T$, where $y_t \in \mathbb{R}^{V \times C}$. In this context, V denotes the number of vertices, and C the feature dimension of the skeletal pose data. Rather than directly modeling $p(y|x)$, we introduce an intermediary representation z , composed of discrete tokens. These tokens capture both spatial and temporal attributes of SL. The generation process can be described by the joint distribution $p(y, z|x) = q(y|z, x)p(z|x)$. Here, $p(z|x)$ denotes the probability of generating the discrete representation z from the input x , while $q(y|z, x)$ represents the probability of generating the continuous signing sequence y based on z and x . The first term is handled by a Vector Quantization (VQ) model, and the second is modeled autoregressively.

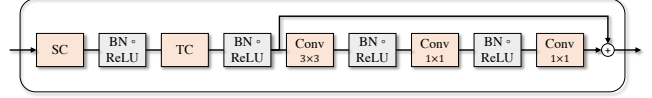


Fig. 2. An overview of the STGP block. Spatial Convolution (SC) and Temporal Convolution (TC) process the input spatially and temporally, respectively, and the subsampled output preserves spatio-temporal features through a resblock. BN refers to Batch Normalize.

Further details of these components are elaborated upon in the following sections.

Discrete Representation of Signing. To convert continuous sign pose sequences into discrete tokens, we introduce Spatio-Temporal Graph Pyramid-based dVAE [14]. It comprises an STGP encoder and decoder as illustrated in Fig. 1. We designed STGP to address the intricacies of down-sampling and up-sampling within a skeleton graph, which features non-uniform grids. This design is inspired by the Graph Pyramid [15]. As shown in Fig. 2, STGP sequentially processes input sequences, catering to both their spatial and temporal aspects. Each processing phase culminates with a resblock, ensuring the retention of down-sampled spatio-temporal information.

This model is tailored to handle fixed-length sign pose sequences represented as $y^{(\ell)} \in \mathbb{R}^{L \times V \times C}$, where L represents the window size. Central to the STGP-dVAE is a codebook comprising latent variable categories, represented as $e_i \in \mathbb{R}^{K \times D_c}$. Here, K signifies the number of latent variable categories, while D_c refers to the embedding size.

For the discretization of the STGP encoder output, we utilize the Gumbel-Softmax relaxation [12]. This method samples a latent from the output of the encoder e_i as:

$$w_i = \frac{\exp(\log(e_i) + g_i)/\tau}{\sum_{k=1}^K \exp(\log(e_k) + g_k)/\tau}, \quad (1)$$

where g_i is the independent i^{th} sample from the Gumbel distribution. The parameter τ adjusts the approximation to the categorical distribution, and w_i represents weights over the codebook vectors. The resulting sampled latent vector is $z^{(\ell)} = \sum_{k=1}^K w_k e_k$.

The model is optimized by minimizing the combined loss function comprising L2 and diversity loss [16]. The L2 loss is defined as

$$\mathcal{L}_{pose} = \frac{1}{L} \sum_{i=1}^L \left\| y_i^{(\ell)} - \hat{y}_i^{(\ell)} \right\|_2^2, \quad (2)$$

where $y^{(\ell)}$ and $\hat{y}^{(\ell)}$ are the ground-truth and predicted poses, respectively. The diversity loss [16] is represented as:

$$\mathcal{L}_{div} = - \sum_{i=1}^K p(e_i) \log(p(e_i)). \quad (3)$$

The final loss can be defined as:

$$\mathcal{L} = \mathcal{L}_{pose} + \alpha \mathcal{L}_{div}, \quad (4)$$

where α is the hyperparameter that determines the scale of diversity loss.

Autoregressive SLP. For the generation of discrete signing tokens from the given textual input, we employ Transformer. Specifically, we employ BERT [17] to extract linguistic features and a Transformer decoder to generate the target output.

As depicted in Fig. 1, before training, the sign pose sequences need to be transformed into discrete tokens. This transformation entails dividing the input sign pose sequence, y , into multiple segments, each spanning length L . Consequently, the output discrete token length becomes $M = \lfloor \frac{T}{L} \rfloor$, resulting in $y \approx \{y_i^{(\ell)}\}_{i=1}^M \in \mathbb{R}^{M \times V \times C}$. For computational efficiency, any remaining sign poses are simply removed. Each segment is subsequently encoded by the pre-trained STGP encoder through the argmax operation, yielding a discrete token denoted as $z_i = \operatorname{argmax}(h_i)$, where h_i is the i^{th} hidden representation from the STGP encoder. To demarcate the start and end of signs, we append z with $\langle \text{bos} \rangle$ and $\langle \text{eos} \rangle$ tokens.

The model is optimized by minimizing a combined loss function, which consists of cross-entropy and latent alignment losses. The cross-entropy loss is represented as:

$$\mathcal{L}_{ce} = - \sum_{i=1}^M \log(p(z_i | z_{<i}, x)), \quad (5)$$

where $p(z_i | z_{<i}, x)$ represents the probability of generating the i^{th} token z_i given the previous tokens $z_{<i}$ and the input x .

The latent loss, employing L2 loss, offers supplementary latent-level signals by aligning the output of the Transformer decoder with that of the STGP encoder. It can be represented as:

$$\mathcal{L}_{latent} = \frac{1}{M} \sum_{i=1}^M \|h_i - \hat{h}_i\|_2^2, \quad (6)$$

where \hat{h}_i is the i^{th} hidden representation from the Transformer decoder.

The overall loss is the sum of the two aforementioned losses:

$$\mathcal{L} = \mathcal{L}_{ce} + \beta \mathcal{L}_{latent}, \quad (7)$$

where β serves as a hyperparameter that scales the latent loss.

4. EXPERIMENTAL SETTINGS

Datasets and Preprocessing. We assess our model using the PHOENIX-2014-T [18] and How2Sign [19] datasets, detailed in Table 1. During preprocessing, skeletal keypoints are normalized to the $[0, 1]$ range. Texts are converted to lowercase and tokenized via BPE-encoding, with vocabulary

	Samples	Max Frame	Min Frame	Avg Frame	FPS
PHOENIX-2014-T [18]	8,257	475	16	116	25
How2Sign [19]	38,611	2,579	32	173	30

Table 1. Statistics of SL Datasets.

	PHOENIX-2014-T			How2Sign		
	FGD↓	DTW-MJE↓	BLEU-4↑	FGD↓	DTW-MJE↓	BLEU-4↑
PT [6]	360.62	0.793	0.59	391.06	0.355	0.57
w/o GN&FP	384.23	0.991	0.73	383.20	0.402	0.33
NSLP-G [8]	150.28	0.638	5.56	291.62	0.327	0.41
w/o Finetuning	179.40	0.646	4.41	440.95	0.321	0.54
SignVQNet	92.64	<u>0.671</u>	6.85	<u>82.76</u>	<u>0.319</u>	0.71
w/o Beam search	<u>96.60</u>	0.670	6.39	81.99	0.317	0.63
Ground-truth	0.0	0.0	8.10	0.0	0.0	0.70

Table 2. Comparison with the states-of-the-art. A lower value (indicated by ↓) is better. The best results are in bold, followed by the second-best in underline. Note: Ground-truth BLEU scores may vary from those in original papers due to differences in implementation, specifically due to the lack of gloss supervision in the SLT model.

sizes set at 3,000 for PHOENIX-2014-T dataset and 10,000 for How2Sign dataset.

Evaluation Metrics. To evaluate the performance of our model, we employ several metrics. We use Back-Translation (BT) [6] to determine the BLEU-4. The DTW-MJE metric, introduced by Huang et al. [9], combines Dynamic Time Warping (DTW) with Mean Joint Error (MJE) to measure discrepancies between predicted and actual signing sequences. Additionally, Fréchet Gesture Distance (FGD) [20] evaluates the visual fidelity of generated sign poses by comparing the distributions of real and generated sequences.

Implementation Details. For our experiments, we utilize the Gumbel-Softmax relaxation and anneal its temperature, τ , from 0.9 down to 0.1. The parameters α and β are set at 0.1 and 0.001, respectively. We use 4 layers of the STGP block. Our Transformer model is configured with a hidden size of 768, comprises 4 layers, and uses 8 attention heads. It also incorporates a dropout rate of 0.1 and an intermediate size of 1,024. We employ the Xavier initialization for our networks and use the AdamW optimizer with a learning rate set at 0.0001. For encoding textual input, we leverage the bert-base-cased and bert-base-german-cased models from HuggingFace, both of which are fine-tuned during training. We select a checkpoint that minimizes the FGD metric for reporting. The entire training process runs for 500 epochs, taking approximately 24 hours on a Tesla A100 GPU, with a batch size of 64.

5. EXPERIMENTAL RESULTS

Comparison to the States-of-the-Art. We conducted a comparative evaluation of our proposed SignVQNet against existing state-of-the-art gloss-free SLP models, as shown in Table 2. To ensure a fair comparison, we adapted the PT

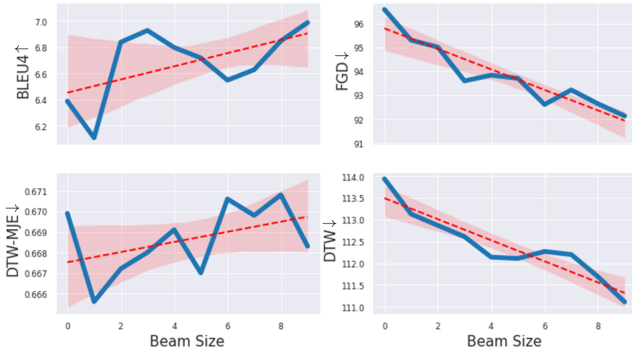


Fig. 3. Performance discrepancy among SLP metrics over the change in performance with different beam sizes.

Window Size	DEV			TEST		
	FGD↓	DTW-MJE↓	BLEU-4↑	FGD↓	DTW-MJE↓	BLEU-4↑
16	42.95	0.310	6.75	41.45	0.301	6.55
32	42.04	0.302	6.77	41.43	0.299	6.88
64	44.68	0.305	6.44	43.21	0.305	6.52

Table 3. Performance comparison with different window sizes.

model to operate without the aid of ground-truth data during inference, as suggested by Huang et al. [9]. Our findings reveal that SignVQNet outperforms its counterparts on both datasets, especially in terms of FGD and BLEU-4 metrics. On the How2Sign dataset, which features longer frame sequences than PHOENIX-2014-T dataset, SignVQNet shows its robustness in generating extended pose sequences. An interesting observation arises from the PHOENIX-2014-T dataset: While SignVQNet outperforms in FGD and BLEU-4, it lags behind NSLP-G in the DTW-MJE metric. We delve deeper into this observation in the subsequent sections.

Analyzing Evaluation Metrics for SLP. Reliable metrics are essential for evaluating generative models in the SLP domain. Currently, the field leans on FGD, DTW-MJE, and BT, but a definitive best metric remains undetermined. As discussed in previous paragraph, these metrics sometimes yield conflicting performance results [21]. To understand these disparities, we examined how varying beam sizes impacts performance on the PHOENIX-2014-T dataset.

Our analysis, as shown in Figure 3, reveals that while FGD and BLEU-4 scores generally benefit from increased beam sizes, DTW-MJE scores exhibit a decline. We also incorporated DTW into our analysis for a holistic perspective. It is worth noting that the DTW-MJE metric, by enforcing alignment between the generated and ground-truth sign pose sequences, might not always provide a true comparison. Specifically, DTW aims to minimize the distance by aligning sequences, which may not always reflect the actual temporal alignment. When combined with MJE, this can lead to inconsistent error measurements.

Ablation Study. We conducted an ablation study using the

Vocab Size	DEV			TEST		
	FGD↓	DTW-MJE↓	BLEU-4↑	FGD↓	DTW-MJE↓	BLEU-4↑
512	42.96	0.315	6.75	41.81	0.312	6.30
1024	42.04	0.302	6.77	41.43	0.299	6.88
2048	44.68	0.306	6.24	44.23	0.306	6.77
4096	56.74	0.325	6.64	55.13	0.323	6.57
8192	55.96	0.317	6.30	55.58	0.315	5.89

Table 4. Performance comparison of different codebook sizes.

Models	DEV			TEST		
	FGD↓	DTW-MJE↓	BLEU-4↑	FGD↓	DTW-MJE↓	BLEU-4↑
GRU	433.76	0.685	0.49	444.74	0.681	0.61
+Attn	383.99	0.697	0.74	402.92	0.700	0.81
Transformer	103.88	0.682	5.33	102.45	0.676	6.22
+BERT [17]	102.87	0.679	6.30	96.51	0.674	5.94

Table 5. Performance comparison of different architectural choices.

Loss	DEV			TEST		
	FGD↓	DTW-MJE↓	BLEU-4↑	FGD↓	DTW-MJE↓	BLEU-4↑
\mathcal{L}_{ce}	102.87	0.679	6.30	96.51	0.674	5.94
\mathcal{L}_{latent}	504.88	0.755	0.36	512.48	0.741	0.40
$\mathcal{L}_{ce} + \mathcal{L}_{latent}$	100.85	0.676	6.76	<u>96.60</u>	0.670	6.39

Table 6. Performance comparison of different losses with \mathcal{L}_{ce} and \mathcal{L}_{latent} .

widely-adopted PHOENIX-2014-T dataset to evaluate the individual contributions of SignVQNet components. First, we gauged the STGP-dVAE’s reconstruction quality, finding an optimal window size of 32 (Table 3). The codebook size was most effective at 1,024 (Table 4). Comparing autoregressive models, Transformers surpassed GRU-based networks, which remain popular for human motion tasks (Table 5). Incorporating BERT further enhanced performance. Our loss function analysis indicated that combining \mathcal{L}_{ce} and \mathcal{L}_{latent} is optimal (Table 6).

Visual Comparisons. We offer a visual comparison of sign pose sequences produced by our SignVQNet in contrast to the baselines¹. Additionally, our supplementary video provides further information, showcasing depictions of words such as “now”, “weather”, and “coming”.

6. CONCLUSION

In this paper, we presented SignVQNet, a novel approach to gloss-free Sign Language Production (SLP) that leverages Vector Quantization to derive discrete tokens from sign pose sequences. This enables genuine autoregression without the need for ground-truth data during inference, addressing the shortcoming of previous autoregressive SLP models. In our experiments, we demonstrate its superiority over prior methods, achieving the state-of-the-art performance on both the PHOENIX-2014-T and How2Sign datasets. Additionally, we highlight the reliability of BT and FGD as evaluation metrics, while noting inconsistencies in the DTW-MJE metric.

¹<http://nlpcl.kaist.ac.kr/projects/signvqnet>

7. REFERENCES

- [1] Mathias Müller, Zifan Jiang, Amit Moryossef, Annette Rios, and Sarah Ebling, “Considerations for meaningful sign language machine translation based on glosses,” in *Proceedings of the 61st Annual Meeting of the Association for Computational Linguistics*, 2023, pp. 682–693.
- [2] Kezhou Lin, Xiaohan Wang, Linchao Zhu, Ke Sun, Bang Zhang, and Yi Yang, “Gloss-free end-to-end sign language translation,” in *Proceedings of the 61st Annual Meeting of the Association for Computational Linguistics*, 2023, pp. 12904–12916.
- [3] Amanda Duarte, Samuel Albanie, Xavier Giró-i Nieto, and Gül Varol, “Sign language video retrieval with free-form textual queries,” in *Proceedings of the IEEE/CVF Conference on Computer Vision and Pattern Recognition*, 2022, pp. 14094–14104.
- [4] Ben Saunders, Necati Cihan Camgoz, and Richard Bowden, “Signing at scale: Learning to co-articulate signs for large-scale photo-realistic sign language production,” in *Proceedings of the IEEE/CVF Conference on Computer Vision and Pattern Recognition*, 2022, pp. 5141–5151.
- [5] Yiting Cheng, Fangyun Wei, Jianmin Bao, Dong Chen, and Wenqiang Zhang, “Cico: Domain-aware sign language retrieval via cross-lingual contrastive learning,” in *Proceedings of the IEEE/CVF Conference on Computer Vision and Pattern Recognition*, 2023, pp. 19016–19026.
- [6] Ben Saunders, Necati Cihan Camgoz, and Richard Bowden, “Progressive transformers for end-to-end sign language production,” in *Proceedings of the 16th European Conference on Computer Vision*. Springer, 2020, pp. 687–705.
- [7] Ben Saunders, Necati Cihan Camgoz, and Richard Bowden, “Mixed signals: Sign language production via a mixture of motion primitives,” in *Proceedings of the IEEE/CVF International Conference on Computer Vision*, 2021, pp. 1919–1929.
- [8] Eui Jun Hwang, Jung-Ho Kim, and Jong C Park, “Non-autoregressive sign language production with gaussian space,” in *Proceedings of the 32nd British Machine Vision Conference*, 2021, pp. 22–25.
- [9] Wencan Huang, Wenwen Pan, Zhou Zhao, and Qi Tian, “Towards fast and high-quality sign language production,” in *Proceedings of the 29th ACM International Conference on Multimedia*, 2021, pp. 3172–3181.
- [10] Ben Saunders, Necati Cihan Camgoz, and Richard Bowden, “Adversarial training for multi-channel sign language production,” in *Proceedings of the 31st British Machine Vision Conference*, 2020, pp. 7–10.
- [11] Chris J Maddison, Andriy Mnih, and Yee Whye Teh, “The concrete distribution: A continuous relaxation of discrete random variables,” *arXiv preprint arXiv:1611.00712*, 2016.
- [12] Eric Jang, Shixiang Gu, and Ben Poole, “Categorical reparameterization with gumbel-softmax,” *arXiv preprint arXiv:1611.01144*, 2016.
- [13] Aaron Van Den Oord, Oriol Vinyals, et al., “Neural discrete representation learning,” *Advances in Neural Information Processing Systems*, vol. 30, 2017.
- [14] Aditya Ramesh, Mikhail Pavlov, Gabriel Goh, Scott Gray, Chelsea Voss, Alec Radford, Mark Chen, and Ilya Sutskever, “Zero-shot text-to-image generation,” in *International Conference on Machine Learning*, 2021, pp. 8821–8831.
- [15] Sijie Yan, Zhizhong Li, Yuanjun Xiong, Huahan Yan, and Dahua Lin, “Convolutional sequence generation for skeleton-based action synthesis,” in *Proceedings of the IEEE/CVF International Conference on Computer Vision*, 2019, pp. 4394–4402.
- [16] Alexei Baevski, Yuhao Zhou, Abdelrahman Mohamed, and Michael Auli, “wav2vec 2.0: A framework for self-supervised learning of speech representations,” *Advances in Neural Information Processing Systems*, vol. 33, pp. 12449–12460, 2020.
- [17] Jacob Devlin, Ming-Wei Chang, Kenton Lee, and Kristina Toutanova, “BERT: Pre-training of deep bidirectional transformers for language understanding,” in *Proceedings of the 2019 Conference of the North American Chapter of the Association for Computational Linguistics: Human Language Technologies*, 2019.
- [18] Necati Cihan Camgoz, Simon Hadfield, Oscar Koller, Hermann Ney, and Richard Bowden, “Neural sign language translation,” in *Proceedings of the IEEE Conference on Computer Vision and Pattern Recognition*, 2018, pp. 7784–7793.
- [19] Amanda Duarte, Shruti Palaskar, Lucas Ventura, Deepti Ghadiyaram, Kenneth DeHaan, Florian Metze, Jordi Torres, and Xavier Giro-i Nieto, “How2sign: A large-scale multimodal dataset for continuous american sign language,” in *Proceedings of the IEEE/CVF Conference on Computer Vision and Pattern Recognition*, 2021, pp. 2735–2744.
- [20] Youngwoo Yoon, Bok Cha, Joo-Haeng Lee, Minsu Jang, Jaeyeon Lee, Jaehong Kim, and Geehyuk Lee, “Speech Gesture Generation from the Trimodal Context of Text, Audio, and Speaker Identity,” *ACM Transactions on Graphics (TOG)*, vol. 39, no. 6, pp. 1–16, 2020.
- [21] Rotem Shalev Arkushin, Amit Moryossef, and Ohad Fried, “Ham2pose: Animating sign language notation into pose sequences,” in *Proceedings of the IEEE/CVF Conference on Computer Vision and Pattern Recognition*, 2023, pp. 21046–21056.